

*Full Length Research Paper*

# Localization of ginsenoside-Rb1 in *Panax ginseng* revealed by immunofluorescence and immunoelectron microscopic techniques

Sadaki Yokota<sup>1\*</sup>, Yuko Onohara<sup>1</sup>, Takuhiro Uto<sup>2</sup>, Hiroyuki Tanaka<sup>3</sup>, Osamu Morinaga<sup>2</sup> and Yukihiro Shoyama<sup>2</sup>

<sup>1</sup> Section of Functional Morphology, Faculty of Pharmaceutical Sciences, Nagasaki International University, Sasebo, Nagasaki, 859-3298, Japan.

<sup>2</sup> Department of Pharmacognosy, Faculty of Pharmaceutical Sciences, Nagasaki International University, Sasebo, Nagasaki, 859-3298, Japan.

<sup>3</sup> Department of Pharmacognosy, Graduate School of Pharmaceutical Sciences, Kyushu University, Fukuoka 812-8582, Japan.

Accepted 19 April, 2011

**Information on the specific location of the medicinal substance ginsenoside-Rb1 (G-Rb1) in Ginseng, *Panax ginseng*, is crucial to obtain the efficient extract of G-Rb1 or to culture G-Rb1 producing cells. In this paper we describe the localization of G-Rb1 in various parts of the plant revealed by immunofluorescence (IF) and immunoelectron microscopy (IEM). IF observations show that G-Rb1 is localized in chloroplasts, peroxisomes and cytoplasm but not mitochondria and vacuoles of leaf parenchymal cells. In the leaf stem, G-Rb1 is localized to vascular bundles as well as vacuoles. In the root, vacuoles of parenchymal cells are stained at various intensities. IEM observations indicate that gold particles showing G-Rb1 antigenic sites are present in the compartments stained by IF technique. In addition, G-Rb1 is localized to the sieve elements of phloem and degrading primary cell wall of xylem and in the root parenchymal cells G-Rb1 is associated with vacuolar protein granules but not in starch granules. The results suggest that G-Rb1 is synthesized in leaf parenchymal cells, transported to the root and stored in vacuoles of these cells.**

**Key words:** *Panax ginseng*, ginsenosides, immunofluorescence, immunoelectron microscopy, chloroplasts, peroxisomes, vacuoles.

## INTRODUCTION

Ginseng, the crude drug mixture of *Panax ginseng* root is one of the most important and widely used herbal medicines in traditional Chinese medicine (TCM). It has been used to enhance stamina and capacity to cope with fatigue and physical stress. The major active components

are the ginsenosides, which consist of protopanaxatriol and/or protopanaxadiol, which possess a dammarane skeleton in their molecular structure. It is well known that the concentration of ginsenosides vary in the ginseng root, and the amount obtained from the root extracts depends on the method of extraction, subsequent treatment (Kitagawa et al., 1989), or even the season of its collection (Tanaka, 1989). Therefore, standardization is urgently required. In order to control the quality of medicinal plants prescribed in TCM, we reported previously a method for the preparation of anti-G-Rb1 and anti-G-Re monoclonal antibodies (mAbs) (Tanaka et al., 1999; Fukuda et al., 2000a) and confirmed that the anti-G-Rb1 mAb was highly specific against G-Rb1 (Tanaka et al., 1999).

\*Corresponding author. E-mail: [syokota@niu.ac.jp](mailto:syokota@niu.ac.jp) Tel: +81 956 20 5638. Fax: +81 956 20 5622.

**Abbreviations:** IF, immunofluorescence; IEM, immunoelectron microscopy; EM, electron microscopy; REM, routine electron microscopy; mAbs, monoclonal antibodies; VG, vacuolar protein granule; TCM, traditional Chinese medicine.

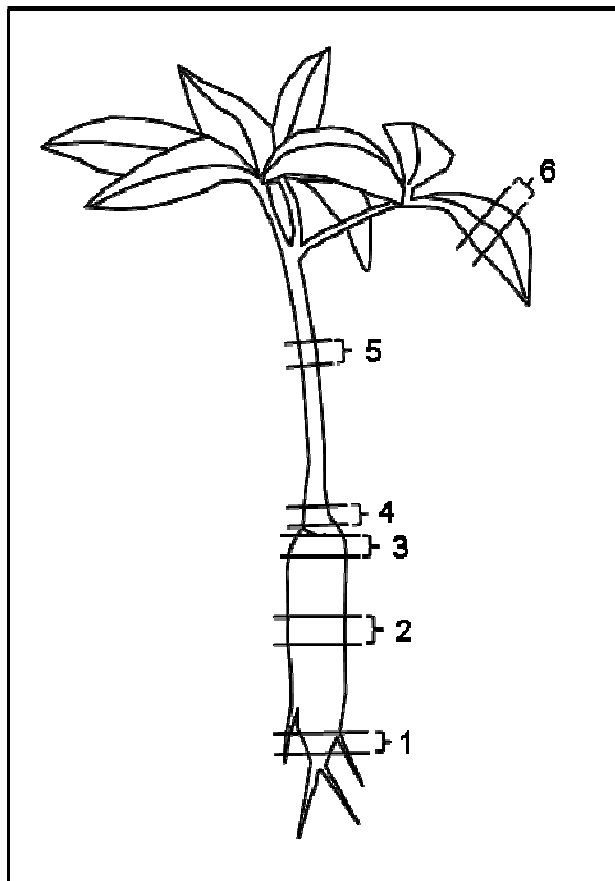


**Figure 1.** An illustration of the areas sampled for staining. These are the; 1) tip region, 2) middle portion, 3) root emergence, 4) rhizome, 5) middle portion of the leaf stem and 6) middle portion of the leaf.

Furthermore, we set up an ELISA and an immunoaffinity concentration method for the one-step isolation of G-Rb1 (Fukuda et al., 2000b). With regard to the distribution of  $\beta$ -glucuronidase (Matsuda et al., 2000), which is a responsive enzyme against oxidation (Sasaki et al., 2000) that is obtained from the TCM herb *Scutellaria baicalensis*, root and stem slices were stained for  $\beta$ -glucuronidase activity using 5-bromo-4-chloro-3-indole- $\beta$ -glucuronide as the substrate.

Clear differences in the distribution of  $\beta$ -glucuronidase were evident, and varied according to the tissues and cultivation season. More recently, we reported that tetrahydrocannabinolic acid synthase, which is a key enzyme related to the marijuana compound (Sirikantaramas et al., 2004), is exclusively expressed in the secretory cells of glandular trichomes. Transgenic tobacco expressing tetrahydrocannabinolic acid synthase fused to green fluorescent protein exhibited fluorescence in the trichome head corresponding to the storage cavity. These results show that the secretory cells of the glandular trichomes not only secrete marijuana compounds but also serve as a biosynthetic site

(Sirikantaramas et al., 2005). In our ongoing histochemistry-based research, we performed IF and IEM for the localization of G-Rb1 in the ginseng organs such as roots, leaves and stems in order to determine the ginsenoside accumulation sites.

## MATERIALS AND METHODS

### Antibodies and protein A-gold probe

The mouse mAb against G-Rb1 was described previously (Tanaka et al., 1999). The mAb was confirmed to react specifically with G-Rb1. Alexa 568<sup>®</sup> labeled goat anti-mouse IgG was obtained from molecular probes (Eugene, OR). A protein A-gold probe of a particle size of 15 nm particle was prepared as described previously (De Roe et al., 1987).

### Tissue preparation

Ginseng, *P. ginseng*, was grown in an herbal garden managed by our Faculty for 3 years and harvested in April. As shown in Figure 1, the plant was washed with running water and tissue samples were obtained from the: 1) tip region, 2) middle portion, 3) root emergence, 4) rhizome, 5) middle portion of the leaf stem, and 6) middle portion of the leaf.

The tissue blocks of each part were cut into 200  $\mu$ m thick sections in ice-cold fixative using a Vibratome (Vibratome<sup>®</sup> Company, St. Louis, MO) and transferred to the fixative consisting of 4% paraformaldehyde, 5% glutaraldehyde and 0.05 M HEPES-KOH buffer (pH 7.2). Sections were fixed for 1 h at 4°C. Fixed tissue slices were cut into small blocks, washed with PBS three times for 15 min each, and dehydrated with a graded ethanol series at -20°C. Finally the tissue blocks were embedded in LR White. The resin was polymerized under UV light overnight at -20°C and for 6 h at room temperature.

### IF staining

Semi-thin sections (500 nm thick) were cut with a histo-diamond knife equipped with a Reichert Ultracut R ultramicrotome. Sections were mounted on silicon-coated glass slides. Sections were treated 3 times with 0.05% sodium borohydride for 4 min each to eliminate the autofluorescence of the glutaraldehyde used for fixation (Osborn et al., 1978).

To block nonspecific antibody absorption, sections were incubated in 2% fish gelatin-0.1 M glycine-PBS for 30 min, and then overnight with anti-G-Rb1 mAb (0.5  $\mu$ g/ml) at 4°C. Sections were washed with PBS and then incubated with Alexa 568<sup>®</sup> labeled goat anti-mouse IgG for 60 min at room temperature.

After being washed with PBS, sections were mounted with Mowiol<sup>®</sup> 4.88 (Calbiochem-MerkBiosciences, Japan) containing 2% 1, 4-diazabicyclo(2.2.2)octane (DABCO, Sigma-Aldrich, Japan). For immunohistochemical controls, the primary antibody was omitted or sections were incubated with IgG from non-immunized mouse, followed by incubation with the Alexa 568<sup>®</sup> labeled secondary antibody. The sections were examined under Nikon Eclipse E600 fluorescence microscopy (Nikon, Tokyo, Japan). The images were merged using Adobe Photoshop<sup>®</sup> 7.0 to visualize the cell contours.

### Post-embedding IEM

Thin sections of LR white-embedded tissues were cut with a

diamond knife equipped with a Reichert Ultracut R ultramicrotome and mounted on nickel grids.

Sections were treated 4 times with 0.05% sodium borohydride for 4 min each and then with 0.1 M Tris-HCl buffer (pH 8.0) containing 0.1 M glycine for 20 min to mask the free aldehyde group of the glutaraldehyde used for fixation. Sections were incubated with 2% fish gelatin-PBS for 30 min, followed by overnight incubation with anti-G-Rb1 mAb (0.5 µg/ml) at 4°C. Sections were then incubated with a protein A-gold probe with 15 nm gold particles for 30 min at room temperature.

For IEM controls, sections were incubated with IgG solution from a non-immunized mouse instead of the anti-G-Rb1 mAb, or the primary antibody was omitted, followed by 30 min-incubation with the protein A-gold probe. All sections were contrasted with 2% uranyl acetate for 10 min and with lead citrate for 30 s, then washed with ultra pure distilled water. After drying, sections were carbon-coated for 10 s and examined with a Hitachi H7650 electron microscope (Hitachi, Tokyo, Japan) at an acceleration voltage of 80 kV.

### Routine electron microscopy (REM)

The tissue slices of each ginseng plant part were fixed in a fixative consisting of 4% paraformaldehyde, 2% glutaraldehyde and 0.05 M Hepes-KOH buffer (pH 7.4) for 1 h at 4°C. After washing with PBS, the tissue slices were post-fixed with 1% reduced OsO<sub>4</sub> for 1 h at room temperature. The tissue slices were then dehydrated with a graded ethanol series and embedded in Spurr's epoxy resin. Thin sections were contrasted with lead citrate for 5 min and examined under electron microscopy as described earlier.

## RESULTS

### IF staining

#### Leaves

G-Rb1 was detected in all of the examined areas of the Ginseng, *P. ginseng* at various staining intensities. In cross-sections of the leaves, the upper and lower epidermis cells were weakly or not stained for G-Rb1, but the palisade and spongy parenchymal cells were strongly stained for G-Rb1 (Figure 2A). The collateral vascular bundle was also heavily stained (Figure 2A, arrows). The control sections were completely negative and showed no staining (Figure 2B). At a higher magnification, G-Rb1 was localized in the chloroplasts (Figure 2C, arrows) and cytoplasm of parenchymal cells. The strongest staining was noted in peroxisomes (Figure 2C, circles). In the central rib region, a relatively large vascular bundle was observed and stained for G-Rb1 (Figure 2A, dotted circle). In a high powered view of the veins, the cells consisting of phloem were heavily labeled (Figure 2D, arrows).

#### Leaf stems and rhizomes

G-Rb1 staining was noted in cellular chloroplasts in the epidermis, cortex, and outer region of the pith. The

heaviest fluorescence was evident in the vascular bundles (Figure 3A). In a high-powered view of the vascular bundle, sclerenchyma cells, the phloem and xylem were positive for G-Rb1 (Figure 3A). In the xylem region, slit elements and intermediate cells between the xylem tubes were strongly stained for G-Rb1 (Figure 3B, arrows and arrowheads). The parenchymal cells around the pith of the leaf stem and the flattened cells covering the surface of the rhizome were weakly stained for G-Rb1 (Figures 3C and 4A). In the outer region of the pith just adjacent to the vascular bundle, the high-powered view showed several tubular structures comprised of G-Rb1-positive cells (Figure 4B). No positive staining reaction was observed in the immunostained control sections (data not shown). Similar results were obtained for the rhizome. The vascular bundles were larger than those found in the leaf stem and the staining intensity was somewhat stronger than in the leaf stem.

### Tip region, middle portion and root emergence

The staining intensity in three regions mentioned earlier was almost the same. Strong staining was noted in the cells of the cork cambium and epidermis. The epidermal cells were elongated and contained strongly stained dots in the stroma (Figure 4A). The vascular bundles were very weakly stained (Figure 4C) in contrast to those of the leaf stem. Parenchymal cells from the cortical layer to the deep region of the pith were stained for G-Rb1 at various intensities. Tubular structures consisting of several cells were noted in the region below (deeper) the vascular bundles. In the high-powered views, the cells comprising the tubules were evidently different from the surrounding parenchymal cells (Figure 4B). In the stroma of the parenchymal cells, several polymorphic inclusions of different staining intensities and G-Rb1-negative deposits were observed (Figure 4D). No positive reaction was observed in the IF control sections (data not shown).

### IEM staining

#### Leaves

We applied the protein A-gold technique to sections of the LR White-embedded materials of each plant part. Heavy labeling with gold particles indicating G-Rb1 antigenic sites was observed in chloroplasts and peroxisomes, but only a few or none were noted in the cytoplasm, mitochondria and vacuoles of parenchymal cells (Figure 5A). Small electron-dense granules were noted in the chloroplast stroma of REM specimens (Figure 5B). There were clear spots in the LR white-embedded specimen, which were not labeled for G-Rb1 (Figures 5A and C). The peroxisomes, which are characterized by an undulating limiting membrane and homogeneous matrix,

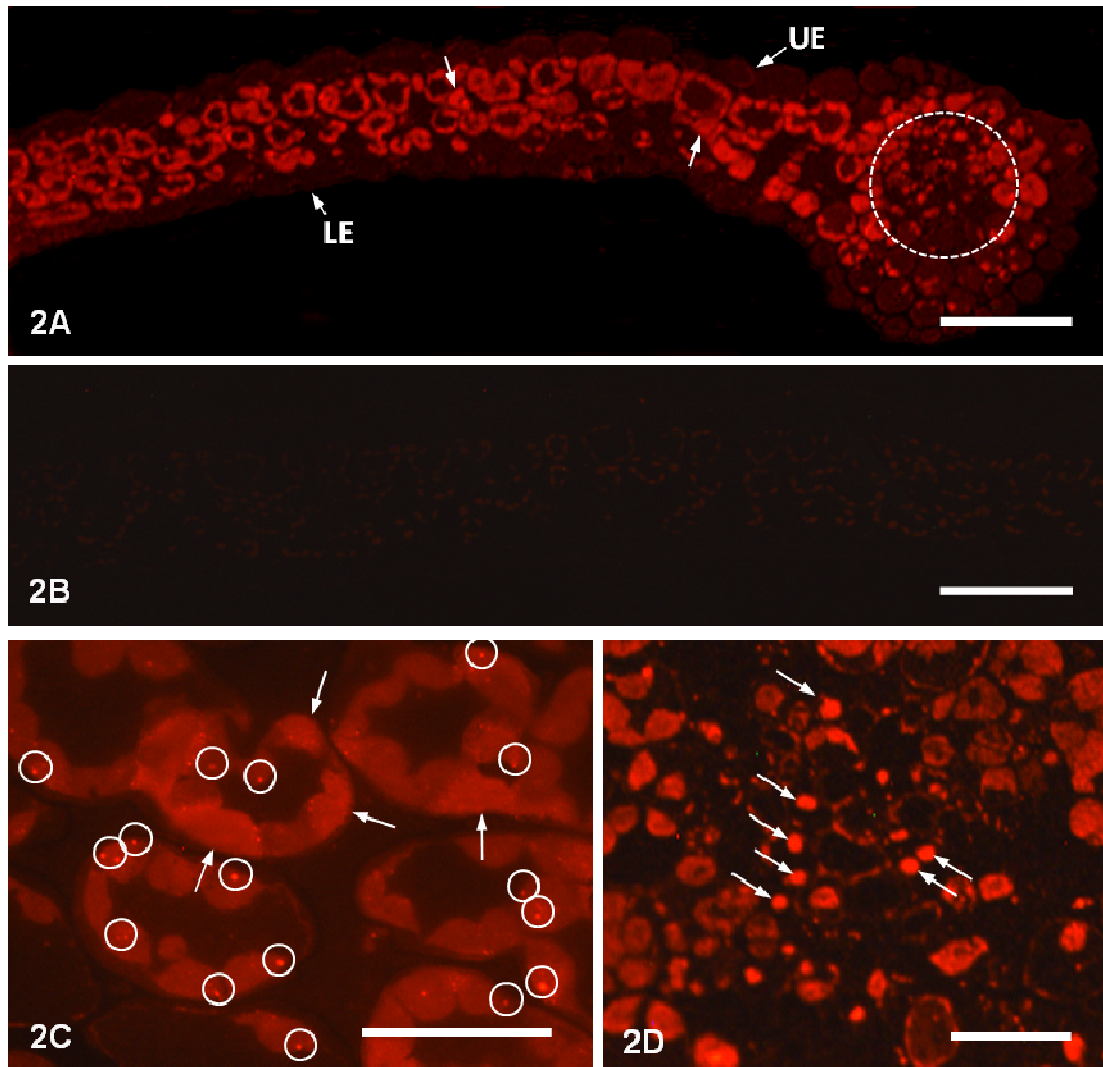


**Figure 2.** Cross-section of a leaf stained by the IF technique. A. low-power view. Note the weak staining or negative staining in cells of the upper epidermis (UE) and lower epidermis (LE). Note also the staining for G-Rb1 in the parenchymal cells and small vascular bundles (arrows). Large central vascular bundle is also positive for G-Rb1 (dotted circle). B. Control section. Note the complete absence of staining. C. Cross-section of a leaf viewed at high magnification. Chloroplasts (arrows) and peroxisomes (circles) of parenchymal cells are strongly stained but vacuoles are not. D. The region of central vascular bundle. Various elements of the leaf veins are stained. The tubule elements of phloem are strongly stained (arrows). Bar = 100  $\mu$ m for A and B, 50  $\mu$ m for C and D.

were frequently observed in leaf parenchymal cells (Figure 5B). In a high-powered view of the peroxisomes, many gold particles were found to be present on electron-dense inclusions (Figure 5D). These gold particles were virtually not present in the control sections incubated with unrelated mouse IgG (Figure 5C). Peroxisomes of companion cells with an attached phloem component were also heavily labeled for G-Rb1 (Figure 5E). Intermediate cells neighboring the vascular elements were strongly labeled (Figure 5F). Furthermore, gold particles were observed in primary cell wall remnants of xylem (Figure 5G).

Cell wall was consistently negative for G-Rb1 (Figures 5F and G).

### Leaf stems and rhizomes

In a substantial proportion of the cortical parenchymal cells, dense and clear granules, the cytoplasm, vacuole and nucleus were stained for G-Rb1 (Figure 6A). The dense granules fused with other small granules (Figure 6A, arrowheads). The content and labeling intensity of the clear granules were quite similar to those of the vacuoles.

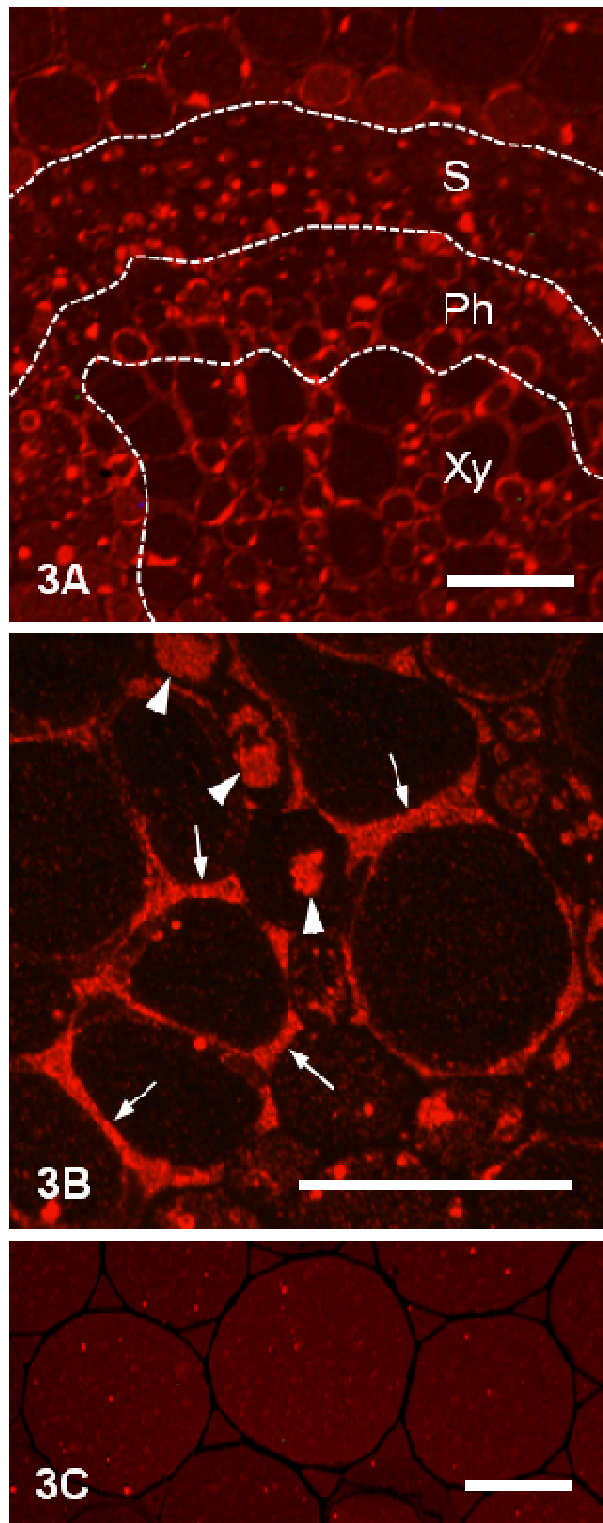


**Figure 3.** A leaf stem immunostained for G-Rb1. A. A vascular bundle of the leaf stem. The sclerenchyma (S), phloem (Ph) and xylem (Xy) are positive for G-Rb1. B. A high magnification view of the xylem. Note the strong staining at the thick boundary between the xylem tubes (arrows) and the intermediate cells between the xylem tubes (arrowheads). C. Parenchymal cells of the pith. Note the staining for G-Rb1 is very weak. Bar = 25  $\mu\text{m}$  for A to C.

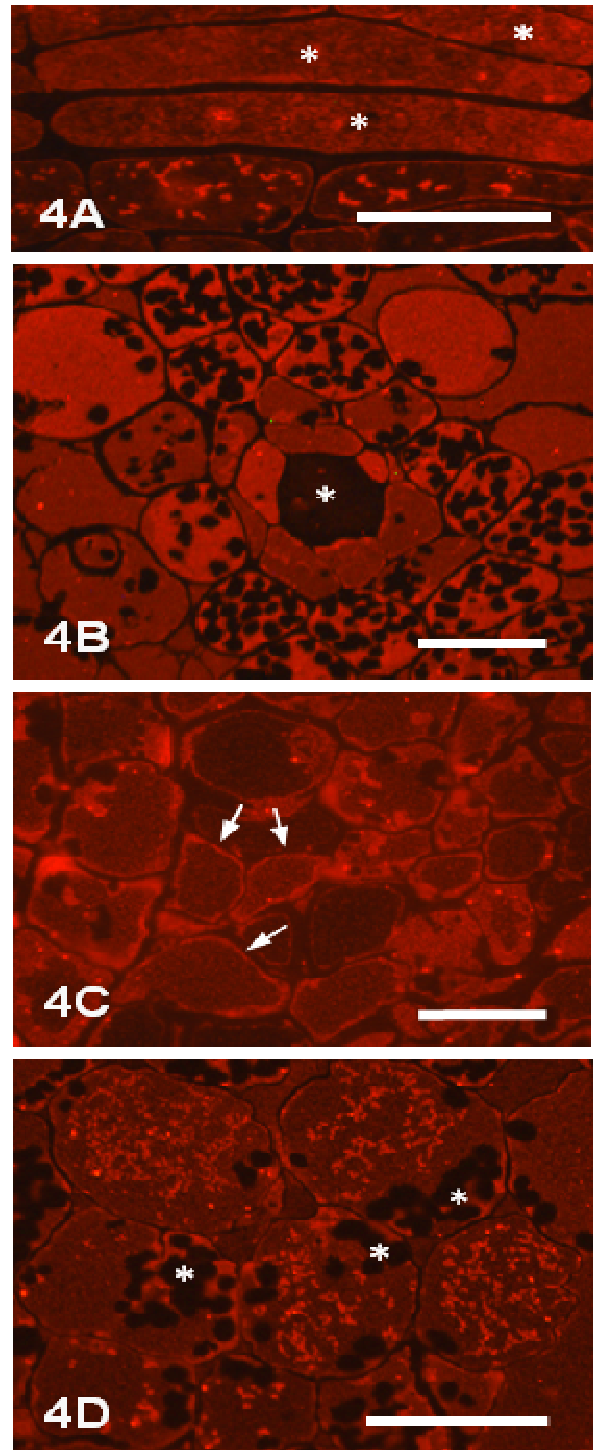


**Figure 4.** Ginseng root immunostained for G-Rb1. A. Elongated cells (\*) in the epidermis. The stroma is stained and contains positive dots. B. A tubular structure (\*) composed of seven cells in this example. The surrounding parenchymal cells are stained for G-Rb1 at various intensities and contain unstained small dark areas displaying starch granules. C. Secondary phloem. Note the staining for G-Rb1 in the phloem fibers (arrows). D. Parenchymal cells in the pith. The stroma contains amorphous structures stained for G-Rb1 and unstained starch granules (\*). Bar = 50  $\mu\text{m}$  for A to D.

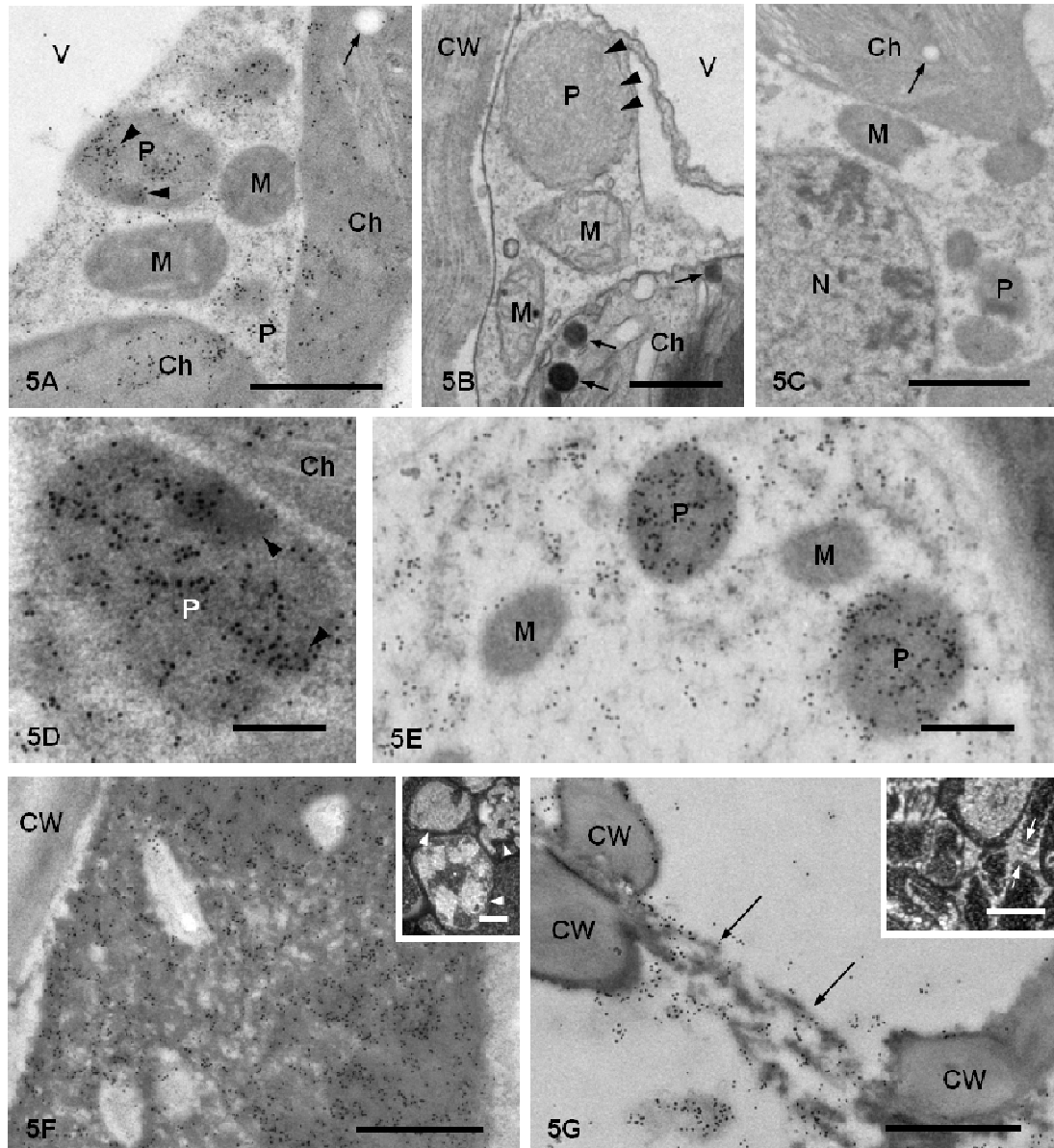


**Figure 5.** IEM of a ginseng leaf and the corresponding IF images. A. A parenchymal cell. Heavy gold labeling for G-Rb1 is observed in the chloroplasts (Ch) and peroxisomes (P) which contain a dense core (arrowheads). The vacuoles (V), mitochondria (M) and cytoplasm are only weakly or not labeled. B. REM of a parenchymal cell. Peroxisomes (P) are characterized by an undulated limiting membrane and homogeneous matrix with inclusions (arrowheads). Mitochondria (M) exhibiting their typical profile. Chloroplasts containing electron dense small granules (arrows). D. A peroxisome (P) at high magnification. Note that gold particles exhibiting G-Rb1 are associated with the dense inclusions (arrowheads). E. A companion cell. G-Rb1 signals are seen in the cytoplasm and peroxisomes (P) but not in mitochondria (M). F. Stroma of an intermediate cell heavily stained for G-Rb1. The corresponding image under IF (arrowheads). G. The sieve element of the phloem. Irregular masses forming the element (arrows) are strongly stained for G-Rb1 but the cell wall (CW) is consistently negative. The corresponding image under IF (arrows). Bar = 1  $\mu$ m for A-C, and E-G, 0.5  $\mu$ m for D and 10  $\mu$ m for upper F and upper G.

The clear large granules fused with each other and sometimes opened a space between the cell and cell wall (Figure 6A). The phloem wall was relatively thick in which the tubule elements were embedded and stained for

G-Rb1 (Figure 6B). Frequently, two or more tube elements were present in a large wall sheath and connected with each other through a narrow canal (Figure 6B). The cytoplasm of the companion cell was

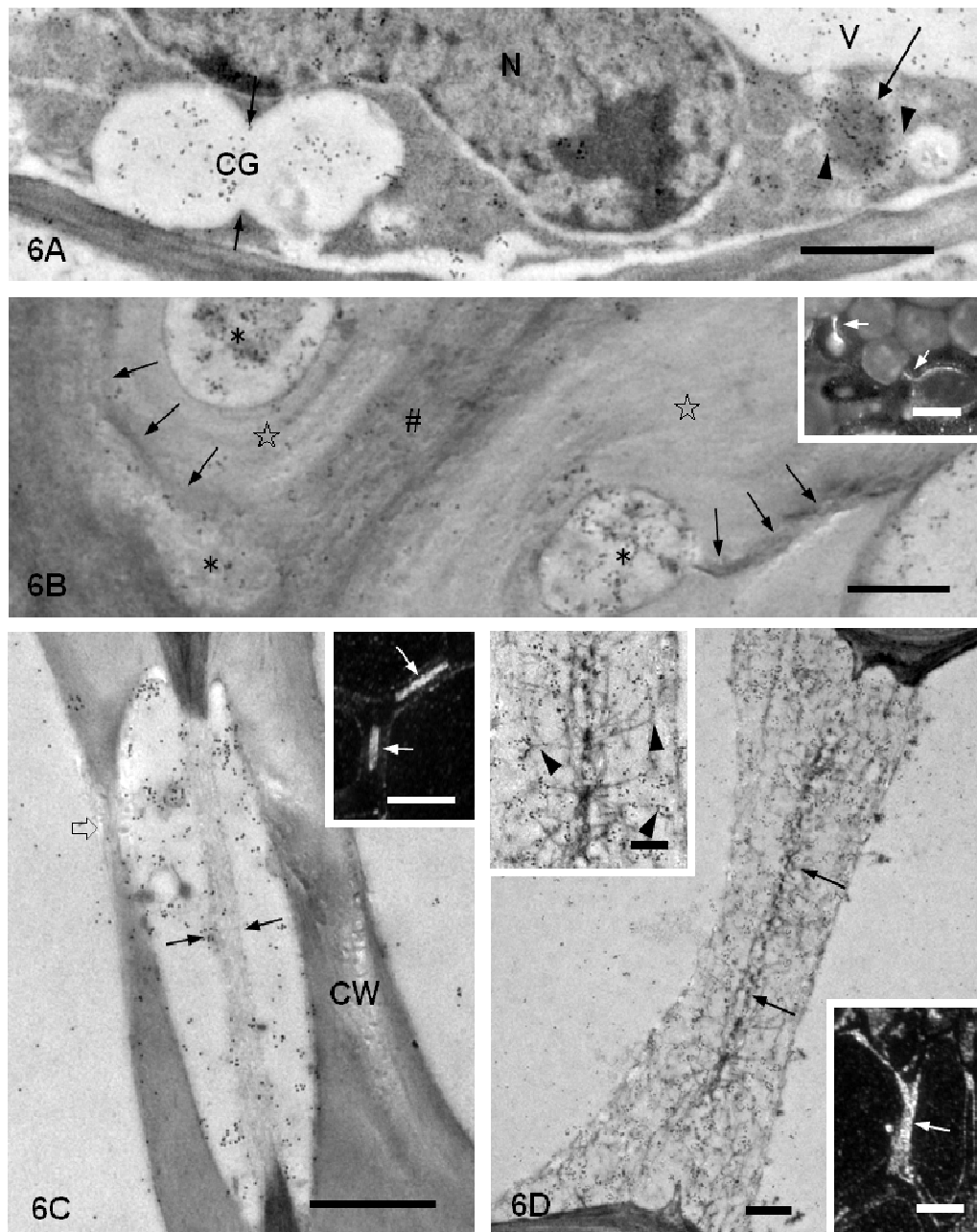


**Figure 6.** IEM localization of G-Rb1 in the leaf stem. A. Cortical parenchymal cells. Note the strong staining for G-Rb1 is in the dense granules (long arrow), clear granules (CG) and vacuoles (V). Note also the fusion of the small granules with the dense granules (arrowheads) as well as the fusion of the clear granules with each other (small arrows). The cytoplasmic matrix and nucleus (N) are weakly labeled. B. Phloem with a thick wall. The tubular element (\*) is heavily stained for G-Rb1. The primary cell wall (#) is weakly stained, but the secondary cell walls (star) are not stained. The tubular elements connect with the other tubules through a canal (arrows). Corresponding IF images. The tubules and canal are stained for G-Rb1 (arrows). C. Perforation of the xylem. Note the disintegration of the dense primary cell wall and the presence of a fine fibrous remnant (arrows). Note also the presence of gold particles in the tubular element surrounded by the secondary cell wall (CW). The latter is disintegrated and has become very thin in the upper left area (open arrow). Corresponding IF image (arrows). D. Perforation between two xylem cells. The primary cell wall has completely disappeared and a fine fibrous mass forms the fibrous remnant, the center of which fibers are concentrated to form a thick mass (arrows). The remnant is strongly labeled for G-Rb1. Upper left. A high-powered view of the fibrous remnant. Fine fibers extend from the central remnant of the primary cell wall (arrowheads). Lower right. Corresponding IF image. The remnant is strongly stained. Bar = 1  $\mu$ m for A to D and D and 10  $\mu$ m for upper B to D and lower D.

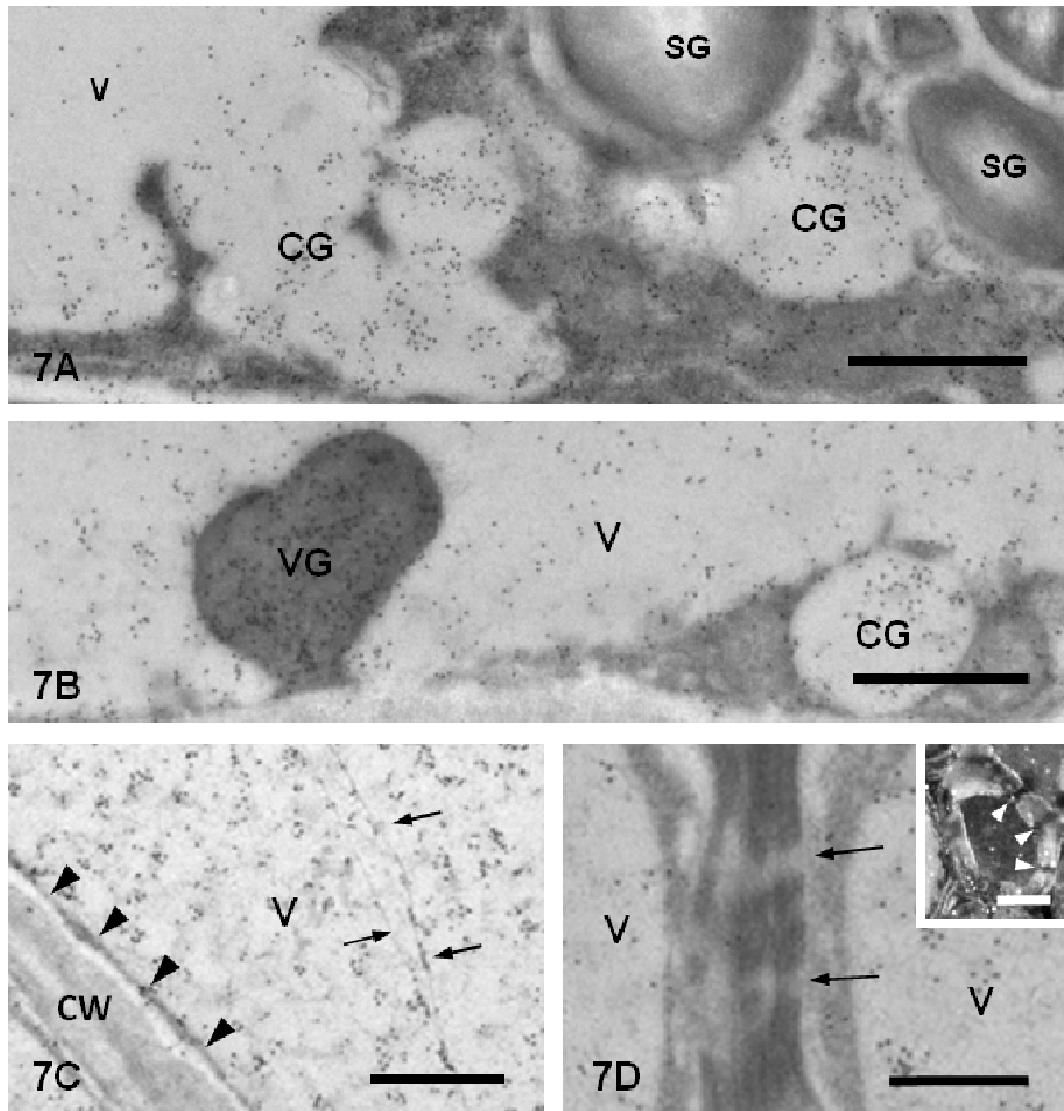


**Figure 7.** IEM localization of G-Rb1 in roots. A. A representative parenchymal cell in the cortical region. The cytoplasmic matrix and clear granules (CG) are heavily stained, but the starch granules (SG) are not labeled by gold particles. The vacuoles (V) intermediately stained. The cell wall (CW) is also not stained. B. Typical parenchymal cells in the pith. Large vacuoles (V). Gold labeling is evident in the vacuoles, clear granules (CG) and vacuolar protein granules (VG) extruding into the vacuoles. C. Parenchymal cells in the pith. Large vacuoles and a thin attenuated cytoplasm are observed (arrowheads). Heavy gold labeling is noted in the vacuoles (V) in which thin fibers are seen (arrows). D. Two parenchymal cells. They communicate with each other through the plasmodesmata (arrows). Gold labeling is present in vacuoles (V) and cytoplasm but not in the cell wall (CW). Corresponding IF image. The plasmodesmata are seen (arrowheads). Bar = 1  $\mu\text{m}$  for A to D and 10  $\mu\text{m}$  for upper D.

Rb1. In the leaf stem, the parenchymal cells of the cortex and pith (are) were stained for G-Rb1. The fine fibrous remnant connected to the primary wall was almost completely negative for G-Rb1 labeling (Figure 6C). However, in the vascular bundles, the degraded primary cell wall remnants of xylem were heavily stained (Figure 6D). The gold particles were associated with fibrils (Figure 6D). The other parts of the xylem tube were weakly or not stained. In addition, the phloem was labeled for G-Rb1 with a similar intensity as that of the leaf stem.

#### **The roots: including the beginning, center and tip regions**

The parenchymal cells of the root were strongly stained. Cells of the cortical region had relatively large cytoplasmic compartments that contained many starch granules (Figure 7A). The vacuole of these cells contained vacuolar protein agglomerates (probably vacuolar protein granules, VG) that were potently stained for G-Rb1 (Figure 7B). Parenchymal cells in the pith

contained large clear granules in the protrusion of narrow cytoplasm, which were strongly stained, frequently fused with each other and opened to the vacuole (Figures 7A and B).

The parenchymal cells were connected with each other through the plasmodesmata (Figure 7D). Almost all of the vacuoles contained numerous starch granules that were consistently negative for G-Rb1. In addition, the vacuoles frequently contained fine fibers in which there were G-Rb1-positive small dense masses (Figure 7C). In the matrix of the vacuoles, various structures, including amorphous masses and protein agglomerate crystalloids were notably stained for G-Rb1 at various intensities (Figures 8A to C). This staining was not observed in the control sections incubated with unrelated mouse IgG (Figure 8D).

## DISCUSSION

### Tissue preparation for the immunostaining of G-Rb1 in *Panax ginseng*

It is evident that G-Rb1 is soluble in water (Zhang et al., 2006). Since the IF procedures are carried out in water, including tissue fixation and the staining reaction, water-soluble substances such as G-Rb1 escape from the tissues during the performance of the procedures. In general, the IEM procedures include mild fixation, dehydration through graded concentrations of ethanol and embedding in resins.

In the IEM procedures, immunostaining reactions are typically performed either after the fixation (pre-embedding technique) (Nakane, 1968) or on thin sections of resin-embedded tissue (post-embedded technique) (Roth, 1982). The pre-embedding technique seems to be not applicable, because G-Rb1 escapes during mild fixation and immunostaining procedures. In the post-embedding technique, the dehydration of tissue by ethanol seems to be a question, because G-Rb1 is soluble in methanol or ethanol (Christensen, 1989). We have tried to apply a freeze-substitution method to the detection of G-Rb1 in the ginseng plant. In this method, fresh tissue is rapidly frozen in liquid nitrogen, the ice in the tissue is substituted by acetone containing glutaraldehyde at  $-80^{\circ}\text{C}$  and finally the tissue is embedded in resin (Harvey, 1982). Immunostaining is carried out on the thin sections of these preparations. Although it is reported that high-pressure freezing of tissues provides good preservation of their biological structure (Dahl and Staehelin, 1989), the preservation of tissue structure was in fact in this case very poor in spite of potent immunostaining for G-Rb1. In the present study, fixation with a high concentration of glutaraldehyde (5%) and dehydration by ethanol at low-temperature ( $-20^{\circ}\text{C}$ ) were applied to plant tissues. Finally, the tissues were embedded in the acryl resin, LR White. We applied the IF technique to semi-thin sections and the protein A-gold

technique to thin sections of the LR White-embedded materials. Thus, we obtained potent immunostaining and good preservation of the cell ultrastructure in the present study.

This is due to the fixation of the tissue using a high concentration of glutaraldehyde and perhaps also the dehydration at the low temperature ( $-20^{\circ}\text{C}$ ). In this regard, nonspecific absorption of IgG into the tissue, which might be caused by the aldehyde radicals of glutaraldehyde, was avoided by treatment of the specimen with sodium borohydride (Osborn et al., 1978) and with glycine-Tris buffer before immunostaining. It is likely that G-Rb1 is trapped in a meshwork of cross-linked proteins and is then finally immobilized in polymerized resin. This is suggested by the fact that it is the very dense vacuolar protein granules which are most heavily stained for G-Rb1. Thus, our data indicate that glutaraldehyde fixation, followed by dehydration at low temperature ( $-20^{\circ}\text{C}$ ), allows the detection of water soluble G-Rb1 in the ginseng tissue.

### IF distribution pattern of G-Rb1 in various plant parts

This study shows that soluble substances such as G-Rb1 can be detected by an IF technique applied to sections of materials that are fixed with a high concentration of glutaraldehyde and embedded in acryl resin, LR white. This method can be used for the localization of other soluble substances. However, in this technique, green fluorescein dye-conjugated secondary antibodies are not used, because acryl resin-embedded biological materials themselves are powerfully fluorescent.

This autofluorescence was reduced using red fluorescein. In addition, autofluorescence due to glutaraldehyde fixation was almost eliminated by sodium borohydride treatment (Osborn et al., 1978). In immunostaining control sections, very weak autofluorescence was noted, especially in chloroplasts and vacuolar protein granules, but the specific staining was much more potent than this vague, general staining. In the present study, strong IF staining for G-Rb1 was observed in the leaves, rhizomes, and roots, with weak staining of the leaf stem of the ginseng plant. Presently, the main root is useful part of resource of ginsenoside, though leaf is not used at all. However, our IF studies found strong staining in the leaf as well as the root, and that is consisted with previous quantitative biochemical analysis of ginsenosides in *P. ginseng* (Yip et al., 1985).

These results suggest that the leaves may nevertheless still be a good resource for production of ginsenosides with various pharmacological effects as pointed out by Yip and coworkers (1985).

### IEM distribution of G-Rb1 and its synthetic sites

The IEM study examination revealed the chloroplasts and

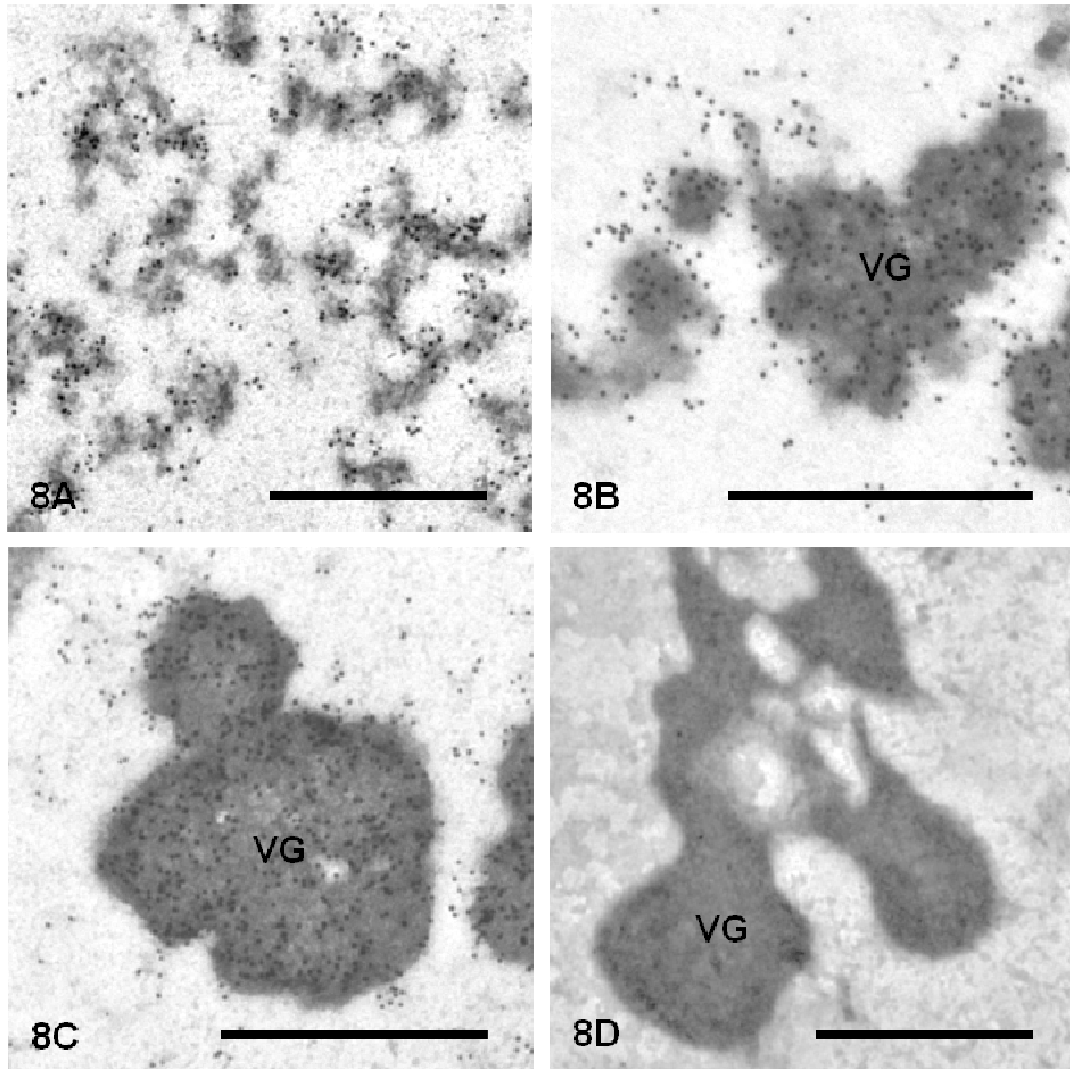


**Figure 8.** G-Rb1-positive inclusions in the vacuoles of the pith parenchymal cells. A. Materials are aggregating in the vacuoles. B. The materials form vacuolar protein granules (VG). C. VG is condensed more compactly. D. Control section incubated with unrelated mouse IgG. Note the lack of staining in the VG. Bar = 1  $\mu$ m for all.

peroxisomes of leaf parenchymal cells to be strongly stained for G-Rb1. In the chloroplasts, the major localization sites for G-Rb1 were noted in the stroma. We recognized by REM that ginseng chloroplasts contained many small dense granules in the stroma, which corresponded to the clear granules in the LR White sections. These granules were almost entirely negative for G-Rb1. Electron dense inclusions were frequently noted in the peroxisome matrix, to which G-Rb1 tended to be localized. These inclusions were observed as weak contours in the Epon sections. The mitochondria and vacuoles of leaf parenchymal cells were weakly or not stained. These results suggested that chloroplasts and peroxisomes are both involved in the biosynthesis of G-Rb1 but mitochondria are not. Weak signals of G-Rb1

were detected in the cytosolic compartment of leaf parenchymal cells so that this compartment cannot be ruled out as a synthetic site for G-Rb1. In the leaf stem, the cells comprising the vascular bundles were strongly stained, but the other parenchymal cells were only weakly stained. This suggests that the G-Rb1 biosynthesized in the leaves is transported to the root via phloem elements. In the root, the contents of the electron lucent cytoplasmic granules and vacuoles, especially the dense VG, were potently stained for G-Rb1. The cytoplasmic granules fused with each other and frequently opened to the vacuoles, suggesting that G-Rb1 which is transported to root parenchymal cells is stored in these granules and released into the vacuoles. In the vacuoles, G-Rb1 seems to be concentrated into VG through certain

aggregation steps. It is not clear whether G-Rb1 chemically binds with proteins in the vacuoles. Strong cross-linking of the proteins with a high concentration of glutaraldehyde might trap G-Rb1 into VG and other dense aggregates so that they become heavily stained for G-Rb1.

Since chloroplasts and peroxisomes are scarce in root parenchymal cells, the G-Rb1 detected in these cells is most likely transported from the leaves rather than synthesized there. It is reported that ginsenosides are biosynthesized via the isoprenoid pathway in the cytosol with mevalonic acid as the precursor for isopentenyl diphosphate and dimethylallyl diphosphate, which are the starting units in the biosynthesis of ginsenosides (Haralampidis et al., 2002; Linsefors et al., 1989; Rohmer 1999). The isoprenoid pathway has been also found in plastids in higher plants (Hoeffler et al., 2002; Kuzuyama, 2002; Roderiguez-Concepcion and Boronat, 2002). It is likely that the cytosolic isoprenoid pathway is present in peroxisomes. However, since this organelle is very labile, it is disrupted and the components are released into the cytosol during biochemical procedures such as homogenization. In fact, more than 60% of peroxisome catalase is released into the cytosol fraction after homogenization in rat liver (Yoshihara et al., 2001). It is thus possible that G-Rb1 is biosynthesized in both peroxisomes and chloroplasts.

## Conclusions

The standard IF technique is applicable to semi-thin Ginseng plant sections fixed by 5% glutaraldehyde and embedded in LR White. By IF, G-Rb1 was localized to parenchymal cells of the leaves and cells in the epidermis, cortex and vascular bundle of the leaf stem. In the root, G-Rb1 was detected in the parenchymal cell vacuoles from the cortex to the pith. A protein A-gold technique can be applied to thin sections of the prepared materials, as described earlier. In the leaf, G-Rb1 was mainly localized in chloroplasts and peroxisomes. In the root, G-Rb1 was detected in the vacuoles of parenchymal cells but not in starch granules. These data suggest that G-Rb1 is biosynthesized in the chloroplasts and peroxisomes within the leaves. The newly biosynthesized G-Rb1 is transported to the root and stored in the vacuoles of root parenchymal cells. This method is clearly potentially applicable to other soluble bioactive natural products in plant tissues.

## ACKNOWLEDGEMENTS

The work is supported by the University research fund and in part by a grant-in-aid (17570158) from the Ministry of Education, Science, Culture and Sport to S.Y. and by the Science Research Promotion Fund from the Promotion and Mutual Aid Corporation for Private

Schools of Japan to Y.S.

## REFERENCES

- Christensen LP (1989). Ginsenosides chemistry, biosynthesis, analysis, and potential health effects. *Adv. Food Nutr. Res.*, 55: 1-99.
- Dahl R, Staehelin LA (1989). High-pressure freezing for the preservation of biological structure: theory and practice. *J. Electron. Microsc. Tech.*, 13(3): 165-174.
- De RC, Courtoy PJ, Baudhuin P (1987). A model of protein-A colloidal gold interactions. *J. Histochem. Cytochem.*, 35(11): 1191-1198
- Fukuda N, Tanaka H, Shoyama Y (2000). Formation of monoclonal antibody against a major ginseng component, ginsenoside Rg1 and its characterization. Monoclonal antibody for a ginseng saponin. *Cytotechnol.*, 34(3): 197-204.
- Fukuda N, Tanaka H, Shoyama Y (2000). Isolation of the pharmacologically active saponin ginsenoside Rb1 from ginseng by immunoaffinity column chromatography. *J. Nat. Prod.*, 63(2): 283-285.
- Haralampidis K, Trojanowska M, Osboum AE (2002). Biosynthesis of triterpenoid saponins in plants. *Adv. Biochem. Eng. Biotechnol.*, 75: 31-49.
- Harvey DM (1982). Freeze substitution. *J. Microsc.*, 127: 209-221.
- Hoeffler JF, Hemmerlin A, Grosdemange BC, Bach TJ, Rohmer M (2002). Isoprenoid biosynthesis in higher plants and in *Escherichia coli*: on the branching in the methylerythritol phosphate pathway and the independent biosynthesis of isopentenyl diphosphate and dimethylallyl diphosphate. *Biochem. J.*, 366: 573-583.
- Kitagawa I, Taniyama T, Yoshikawa M, Ikenishi Y, Nakagawa Y (1989). Chemical Studies on Crude Drug Processing. VI. : Chemical Structures of Malonyl-ginsenosides Rb<sub>1</sub>, Rb<sub>2</sub>, Rc, and Rd Isolated from the Root of *Panax ginseng* C. A. MEYER. *Chem. Pharm. Bull.*, 37: 2961-2970.
- Kuzuyama T (2002). Mevalonate and nonmevalonate pathways for the biosynthesis of isoprene units. *Biosci. Biotechnol. Biochem.*, 66(8): 1619-1627.
- Linsefors L, Björk L, Mosbach K (1989). Influence of elicitors and mevalonic acid on the biosynthesis of ginsenosides in tissue cultures of *Panax ginseng*. *Biochem. Physiol. Pflanz.*, 184: 413-418.
- Matsuda T, Hatano K, Harioka T, Taura, F, Tanaka H, Tateishi N, Shan S, Morimoto S, Shoyama Y (2000) Histochemical investigation of  $\beta$ -glucuronidase in culture cells and regenerated plants of *Scutellaria baicalensis* Georgi. *Plant Cell Rep.*, 19(4): 390-394.
- Nakane PK (1968). Simultaneous localization of multiple tissue antigens using the peroxidase-labeled antibody method: a study of pituitary glands of the rat. *J. Histochem. Cytochem.*, 16(9): 557-560.
- Osborn M, Webster RE, Weber K (1978). Individual microtubules viewed by immunofluorescence and electron microscopy in the same PtK2 cell. *J. Cell. Biol.*, 77(3): R27-34.
- Roderiguez CM, Boronat A (2002). Elucidation of the methylerythritol phosphate pathway for isoprenoid biosynthesis in bacteria and plastids. A metabolic milestone achieved through genomics. *Plant Physiol.*, 130(3): 1079-1089.
- Rohmer M (1999). The discovery of a mevalonate-independent pathway for isoprenoid biosynthesis in bacteria, algae and higher plants. *Nat. Prod. Rep.*, 16(5): 565-574.
- Roth J (1982). The Protein A-Gold (pAg) Technique-A qualitative and quantitative approach for antigen localization on thin sections. In: Bullock GR, Petrusz P (eds) *Techniques in immunocytochemistry*: Academic Press, London, 1: 108-133.
- Sasaki K, Taura F, Shoyama Y, Morimoto S (2000). Molecular characterization of a novel  $\beta$ -glucuronidase from *Scutellaria baicalensis georgi*. *J. Biol. Chem.*, 275(35): 27466-27472.
- Sirikantaramas S, Morimoto S, Shoyama Y, Ishikawa Y, Wada Y, Shoyama Y, Taura F (2004). The gene controlling marijuana psychoactivity: molecular cloning and heterologous expression of Delta1-tetrahydrocannabinolic acid synthase from *Cannabis sativa* L. *J. Biol. Chem.*, 279(38): 39767-39774.
- Sirikantaramas S, Taura F, Tanaka Y, Ishikawa Y, Morimoto S, Shoyama Y (2005). Tetrahydrocannabinolic acid synthase, the enzyme

- controlling marijuana psychoactivity, is secreted into the storage cavity of the glandular trichomes. *Plant Cell Physiol.*, 46(9): 1578-1582.
- Tanaka H, Fukuda N, Shoyama Y (1999). Formation of monoclonal antibody against a major ginseng component, ginsenoside Rb1 and its characterization. *Cytotechnology*, 29(2): 115-120.
- Tanaka O (1989). Saponin composition of *Panax* species. In Shibata S, Ohtsuka Y, Saito H (eds) *Recent advances in ginseng studies*, Hirokawa Publishing Co., Tokyo, pp. 43-47.
- Yip TT, Lau CN, But PP, Kong YC (1985). Quantitative analysis of ginsenosides in fresh *Panax ginseng*. *Am. J. Chin. Med.*, 13(1-4): 77-88.
- Yoshihara T, Hamamoto T, Munakata R, Tajiri R, Ohsumi M, Yokota S (2001). Localization of NADP-dependent isocitrate dehydrogenase in the peroxisomes of rat liver cells. *Biochemical and immunocytochemical studies. J. Histochem. Cytochem.*, 49(9): 1123-1131.
- Zhang S, Chen R, Wu H, Wang C (2006). Ginsenoside extraction from *Panax quinquefolium* L. (American ginseng) root by using ultrahigh pressure. *J. Pharm. Biomed. Anal.*, 41(1): 57-63.